Estimating Depth of Influence of GPR Ground Wave in Lysimeter Experiment

Baby PALLAVI[1], Hirotaka SAITO[1], Makoto KATO[1]

Abstract: To map the surface soil moisture content with GPR at an intermediate scale, the soil dielectric constant needs to be determined from the ground wave velocity.　However, the depth of influence of ground wave is still not well defined.　In the present study, shallow water boxes were placed at near surface (0-20 cm) inside the lysimeter to evaluate the effect on the ground wave and to compare with the theoretical depth of influence using Sperl and Van Overmeeren models.　Results revealed an increase in dielectric constant with all water box measurement until 15 cm depth.　While at 20 cm depth observed K value was found similar as of background soil.　The theoretical prediction of GW depth using both models was found insignificant in the present study.　Experimentally observed result signifies that the depth of influence of GW was similar to the quarter of the wavelength.

Keywords: Depth of influence, Dielectric constant, Ground penetrating radar (GPR), Ground wave

1. Introduction

In agricultural management, spatial distribution of soil moisture content is a key parameter for optimizing crop yields, achieving high irrigation efficiencies, minimizing lost yields due to water logging and salinization (Hubbard *et al*., 2002).　Available techniques to assess spatial variations of the moisture content are either suited to measure small-scale or large-scale variations.　Ground-penetrating radar (GPR) allows one to explore the subsurface in a field scale using electromagnetic (EM) energy at frequencies of 10–1200 MHz (Davis and Annan, 1989).

Among different approaches, the ground wave (GW), one of direct waves recorded in GPR measurements, is of interest in mapping surface soil moistures.　Direct waves are those travel directly from the transmitter to the receiver through the air and along the soil surface.　GW is the one travels along the soil surface.　The advantage of using GW is that, unlike all reflected or refracted waves, the travel distances are known.　However, the sampling volume of GW is still poorly understood, in other words, the depth of influence of GW is not well defined.　Several authors evaluated the depth of influence by comparing water content point estimates measured with TDR probes or gravimetric columns with the GPR measurement (Galagedara *et al*, 2003; Grote *et al*., 2003).　However comparing with point measured moisture content values is very questionable because the measurement volume of GPR is clearly bigger than that of the point measurement.

The main goal of the present study was then to investigate the influence zone of GW using only GPR information.　To estimate the depth of influence of GW, lysimeter experiments were conducted with near surface heterogeneity created by placing a large anomaly near the surface.

2. Materials and Methods
2.1. Lysimeter Setup

A wooden lysimeter (180 × 90 × 90 cm) filled with river sand was used to examine the depth of influence of GW.　The textural class of the soil was sand as determined by the grain size analysis. Different sets of near surface heterogeneity were created by placing shallow plastic boxes filled with water in the centre of the lysimeter at varying (0-20 cm) depths.　Plastic Boxes were used because the dielectric constant is similar to that of the background sand.　Water filled boxes were used because of high contrasts in the dielectric constant with that of the background soil.　As the moisture content in soil increases, the EM velocity decreases.　Water boxes in four different dimensions were used (**Table 1**).　The top view of the experimental setup with Box-I and GPR antennas is depicted in **Figure 1**.　Similar setups were achieved for different boxes changing the placement depth only (0, 5, 10, 15 and 20 cm).　Boxes were
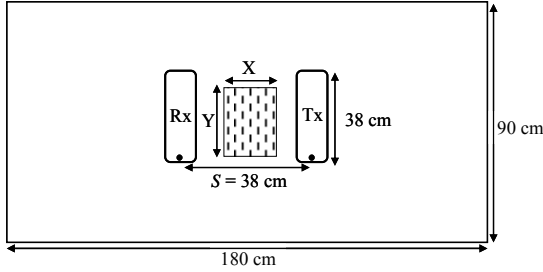
Fig. 1. Schematic top view of the lysimeter with Box-I and antennas placements.

Table 1. Dimensions of water boxes.

Water box	Dimensions (cm) [X; Y; Z]	Area (cm^2)	Volume (cm^3)
Box-I	24 x 31.5 x 2.5	756	1,890
Box-II	48 x 31.5 x 2.5	1,512	3,780
Box-III	24 x 31.5 x 5	756	3,780
Box-IV	12 x 36 x 3.5	432	1,512

always placed in the same manner as shown in Figure 1. When the boxes were placed at 0 cm depth, the upper surface of the box and the soil surface were kept at the same level. The GPR measurements were conducted using a pulseEKKO pro 250 system, which has a 250 MHz central frequency.

2.2. Theoretical Background of GPR

In GPR, the transmitter radiates energy spherically both into air and ground. The receiving antenna subsequently records the modified signals. The wave propagates through the soil is reflected, scattered and attenuated by subsurface dielectric contrasts (**Fig. 2**). The first strong signal usually represents airwave (AW), which travels directly from the transmitter to the receiver through the air at the speed of the EM wave in vacuum. GW travels between the transmitter and the receiver along the soil surface. The propagation velocity of GW (v_{gw}) depends on the dielectric constant of the soil K (in other words, the moisture content θ). The velocity (v_{gw}) is calculated by dividing the antenna separation (S) by the ground wave travel time (GWTT: t_{gw});

$$v_{gw} = \frac{S}{t_{gw}} \qquad (1)$$

The dielectric constant K is then calculated by the following equation (Davis and Annan, 1989),

$$K \approx \left(\frac{c}{v_{gw}}\right)^2 \qquad (2)$$

where c is the speed of the EM wave in vaccum (3×10^8 m/s). The volumetric water content is then obtained from K using one of the empirical models, such as the Topp equation (Topp *et al*., 1980). Two different models have been proposed to calculate the depth of influence of GPR ground wave (D_{gw}). First model is proposed by van Overmeeren *et al*. (1997), who adapted the seismic approximation.

$$D_{gw} = \frac{1}{2}\sqrt{\frac{v_{gw} S}{f}} \qquad (3)$$

The second model is proposed by Sperl (Huisman, 2003),

$$D_{gw} = 0.145\sqrt{\frac{v_{gw}}{f}} \qquad (4)$$

where *f* is the central frequency of GPR (Hz).

2.3. GPR Survey

Two common GPR acquisition approaches; common midpoint (CMP) and common offset (CO), were used in this study.

2.3.1. Common-midpoint (CMP) Approach

In CMP, the separation distance between two antennas are increased in a constant step size, while
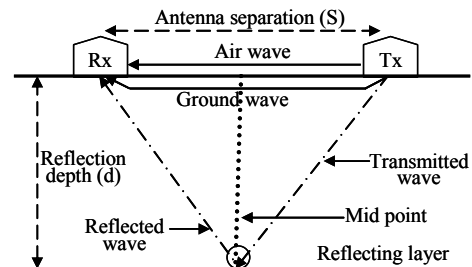
Fig. 2. Schematic diagram of travel path of waves at a single offset (**Lunt** *et al*., 2005)

keeping the mid point common (Fig. 2). As the distance between two antennas increases, the EM wave travel time also increases. The EM wave velocity is then the inverse of the linear slope obtained by plotting GWTT as a function of the antenna separation.

2.3.2. Common-offset (CO) Approach

In CO, two antennas are moved along the survey line by keeping the distance between the transmitter and the receiver constant. This mode is easy to operate, provides rapid measurement and is used widely in mapping purposes. However, proper time-zero calibration is inevitable. Time-zero is defined as the time when EM pulse starts and all other arrival times need to be analyzed with respect to this time. Each GPR system has an inherently defined time zero, but it cannot be directly obtain. Instead, there are approaches to indirectly estimate time-zero. One approach is to use AW (referred to as AW time-zero calibration). Since the true AW travel time (AWTT) can be estimated by dividing the antenna separation by the speed of light, we can readily obtain time zero by subtracting AWTT from the AW pick. This may not be an ideal option as time-zeros for AW and GW are usually different. Another approach, referred to as the CMP time-zero calibration, is then to use the CMP measurement where one can obtain the true GW velocity. From the true velocity, true GWTT can be calculated, which is then subtracted from the GW pick to determine the CMP calibrated time-zero.

3. Results and Discussion

The profile of the lysimeter sand without an anomaly obtained with the CMP survey is shown in **Figure 3** with AW and GW picked. The estimated GW velocity was 0.16 mns^{-1}, which was converted to dielectric constant ($K= 3.53$) using Eq. (2). Point measurements were also made using the gravimetric method and soil moisture sensors to compare with GPR data. All these point measurements gave the volumetric water content estimates, which were converted to dielectric constants using the Topp equation. The estimated dielectric constant of 3.17 from reference point measurements showed a small difference with that obtained from the CMP survey. The moisture content for $K= 3.17$ corresponds to 0.034 m^{3}m^{-3} and that for $K= 3.53$ corresponds to 0.043 m^{3}m^{-3} based on the Topp equation.

In the next experiment, measurements with water boxes were conducted. The CO survey with a 0.38-m antenna separation was conducted to observe the response of an anomaly on the single trace data. The single trace data of the sand and the sand with Box-I are given in **Figure 4**. The first strong trough (minimum amplitude) was picked as AW, while the next minimum for the GW. The amplitude of AW for the sand and the sand with Box-I was same as expected, but amplitudes were different between the two for GW and others due to the existence of the anomaly. The GWTT of the sand collected from raw data of the CO survey was 5.48 ns, whereas that corrected by the AW time zero was 4.09 ns and that corrected by the CMP time zero was 2.38 ns. As the CMP survey gives more accurate information, the CMP calibrated time zero was used to calculate the velocity and the dielectric constant for all anomaly setups in the remainder of the paper.

The estimated dielectric constants for all four boxes placed at the depth of 0 to 20 cm inside the lysimeter are shown in **Figure 5**. For Box-I, a 0.04 ns increase in GWTT from the sand without box was observed. This increase led the dielectric constant of the surface soil to 4.85 that corresponds to the
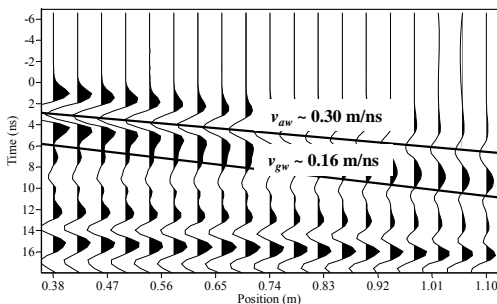
Fig. 3. Wiggle trace of the sand profile with AW & GW velocity.
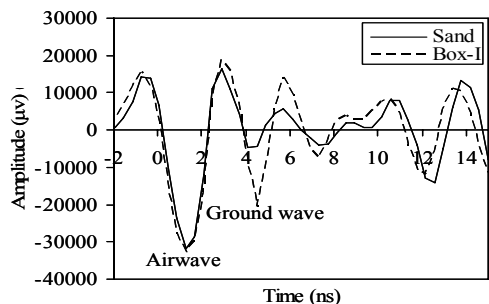
Fig. 4. Early time (-2 to 10 ns) single wavelets acquired for sand and sand with water Box-I.
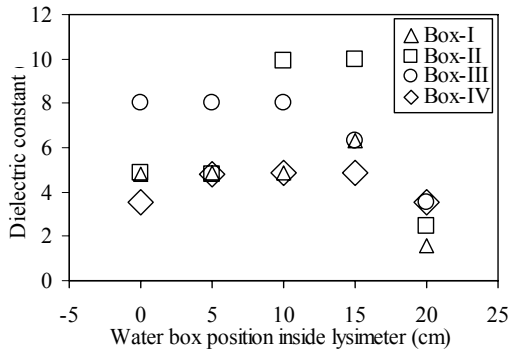
Fig. 5. Measured dielectric constant with water box placement (0-20 cm) inside lysimeter.
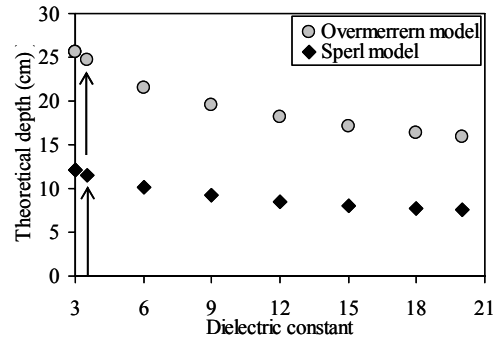
Fig. 6. Theoretical depth of influence of GW for material (K= 3 to 20) using 250 MHz antenna.

moisture content of 0.075 $m^3 m^{-3}$ based on the Topp equation. Then a slight increase in K value was found for the 15 cm placement. Similarly, for the Box-II, estimated K values were smaller for 0 and 5 cm placement (*K*= 4.85) than those for 10 and 15 cm placements (*K*= 9.92). For Box-III, the K values were larger than those obtained for Box-I and Box-II experiments when boxes were placed in shallow depth. The *K* value decreased for the 15-cm placement. Comparison between Box-II and Box-III reveal that boxes with the same volume but with the different surface areas resulted in different *K* values. The *K* value is larger for the box with a larger surface area. The *K* values were almost constant for Box-IV regardless of its placement depth. This might be due to the small surface area of the water box (Table 1). It is therefore clear that the GW is influenced not only by the volume of water but also by the surface area of the box. Overall, it can be said that, except for Box-IV, boxes were imaged by GW until 15 cm depth. At the depth of 20 cm, the estimated dielectric constants are all similar to that of the background sand for all four boxes. This result suggests that the depth of influence of GW in this study was smaller than 20 cm.

The theoretical depths of influence of GW were then calculated using van Overmeeren (1997) and Sperl (Huisman, 2003) models. Predicted depths for the materials (*K*= 3 to 20) using 250 MHz GPR antenna by both models were given in **Figure 6**. In general, the van Overmeeren model predicts larger depths than the Sperl model (Fig. 6). The depth of influence of GW for the background sand was calculated 25 and 12 cm (shown by arrows in Fig. 6), respectively. In this study, all observed depths of influence were less than 20 cm but greater than 15 cm. The theoretical prediction of GW depth using both models does not match with experimental results. The depth of influence was found similar to the quarter of wavelength 16 cm (e.g., D_{gw}= (λ/4); where, λ = (v_{gw}/f) = (16 cmns^{-1}/250×10^6) = 64 cm) in this study. In conclusion, the study signifies that when working with GW of GPR, the CO survey followed by time zero calibration by the CMP survey would provide precise travel time information. Accordingly, the GW velocity can be used to map surface soil moisture contents with the known sampling volume.

References

Davis J.L., Annan A.P. (1989): Ground-penetrating radar for high resolution mapping of soil and rock stratigraphy. *Geophysical Prospect*, **37**: 531-551.

Galagedara L.W., Parkin G.W., Readman J.D. (2003): An analysis of the ground-penetrating radar direct ground wave method for soil water content measurement. *Hydrol. Process*, **17**: 3615–3628.

Grote K., Hubbard S., Rubin Y. (2003): Field-scale estimation of volumetric water content using GPR ground wave techniques. *Wat. Resour. Res.*, **39**: 1321–1335.

Hubbard S., Grote K,m Rubin Y. (2002): Mappting the volumetric soil water content of a California vineyard using high-frequency GPR ground wave data. *Leading Edge*, **21**: 552-558

Huisman J.A., Hubbard S.S., Readman J.D., Annan A.P. (2003): Measuring soil water content with ground penetrating radar: A review. *Vadose Zone J.*, **2**: 476–491.

Topp G.C., Davis J.L., Annan A.D. (1980): Electromagnetic determination of soil water content: measurements in coaxial transmission lines. *Wat. Resour. Res.*, **16**: 574-582.

Van Overmeeren R.A., Sariowan S.V., Gehreis J.C. (1997): Ground penetrating radar for determining volumetric soil water content; results of comparative measurements at two sites. *J. Hydrol.*, **197**: 316– 338.